Divergent Tumor Necrosis Factor Receptor–Related Remodeling Responses in Heart Failure

Role of Nuclear Factor-κB and Inflammatory Activation

Tariq Hamid, PhD; Yan Gu, MD, PhD; Roger V. Ortines, BS; Chhandashri Bhattacharya, MS; Guangwu Wang, MD, PhD; Yu-Ting Xuan, PhD; Sumanth D. Prabhu, MD

Background—Although preclinical data suggested that tumor necrosis factor-α (TNF) neutralization in heart failure (HF) would be beneficial, clinical trials of TNF antagonists were paradoxically negative. We hypothesized that TNF induces opposing inflammatory and remodeling responses in HF that are TNF-receptor (TNFR) specific.

Methods and Results—HF was induced in wild-type (WT), TNFR1$^{-/-}$, and TNFR2$^{-/-}$ mice via coronary ligation. Compared with WT HF, 4-week postinfarction survival was significantly improved in both TNFR1$^{-/-}$ and TNFR2$^{-/-}$ HF. Compared with sham, WT HF hearts exhibited significant remodeling with robust activation of nuclear factor (NF)-κB, p38 mitogen-activated protein kinase, and JNK2 and upregulation of TNF, interleukin (IL)-1β, IL-6, and IL-10. Compared with WT HF, TNFR1$^{-/-}$ HF exhibited (1) improved remodeling, hypertrophy, and contractile function; (2) less apoptosis; and (3) diminished NF-κB, p38 mitogen-activated protein kinase, and JNK2 activation and cytokine expression. In contrast, TNFR2$^{-/-}$ HF showed exaggerated remodeling and hypertrophy, increased border zone fibrosis, augmented NF-κB and p38 mitogen-activated protein kinase activation, higher IL-1β and IL-6 gene expression, greater activated macrophages, and greater apoptosis. Oxidative stress and diastolic function were improved in both TNFR1$^{-/-}$and TNFR2$^{-/-}$ HF. In H9c2 cardiomyocytes, sustained NF-κB activation was proapoptotic, an effect dependent on TNFR1 signaling, whereas TNFR2 overexpression attenuated TNF-induced NF-κB activation.

Conclusions—TNFR1 and TNFR2 have disparate and opposing effects on remodeling, hypertrophy, NF-κB, inflammation, and apoptosis in HF: TNFR1 exacerbates, whereas TNFR2 ameliorates, these events. However, signaling through both receptors is required to induce diastolic dysfunction and oxidative stress. TNFR-specific effects in HF should be considered when therapeutic anti-TNF strategies are developed. **(*Circulation*. 2009;119:1386-1397.)**

Key Words: heart failure ■ inflammation ■ remodeling ■ tumor necrosis factor

Circulating levels of tumor necrosis factor-α (TNF) and soluble TNF receptors (TNFRs) are independent predictors of mortality in patients with heart failure (HF).[1] TNF antagonism is cardioprotective in rats subjected to continuous TNF infusion,[2] in mice with cardiac-restricted TNF overexpression,[3] and in experimental animal models of HF.[4,5] These and other studies suggested that TNF blockade in HF would result in clinical improvement. Surprisingly, however, randomized trials of anti-TNF therapy in human HF failed to show benefit and unexpectedly demonstrated a time- and dose-related increase in death and HF hospitalization.[1] Hence, whether or not TNF is a viable therapeutic target in HF remains largely unresolved.

Editorial p 1355
Clinical Perspective p 1397

The paradoxical clinical trial results implied a more complicated role for TNF in HF than is currently considered. Indeed, TNF-mediated effects are not uniformly detrimental in the heart. As a stress-response protein, TNF is cytoprotective during conditions such as ischemic injury,[6] coronary microembolization,[7] and infectious myocarditis.[8] TNF signaling occurs via 2 cell-surface receptors (TNFR1 and TNFR2) and in large part via the TNFR-associated factor 2 (TRAF2)–dependent activation of nuclear factor (NF)-κB, p38 mitogen-activated protein kinase (MAPK), and c-Jun N-terminal kinase (JNK).[9] We tested the hypothesis that TNF induces dichotomous effects in HF on the basis of the relative

Received June 27, 2008; accepted December 19, 2008.

From the Institute of Molecular Cardiology, Department of Medicine, University of Louisville and Louisville Veterans Affairs Medical Center, Louisville, Ky.

The online-only Data Supplement is available with this article at http://circ.ahajournals.org/cgi/content/full/CIRCULATIONAHA.108.802918/DC1.

Correspondence to Sumanth D. Prabhu, MD, Department of Medicine/Cardiovascular Medicine, University of Louisville, ACB, 3rd Floor, 550 S Jackson St, Louisville, KY 40202. E-mail sprabhu@louisville.edu

Circulation **is available at http://circ.ahajournals.org** **DOI: 10.1161/CIRCULATIONAHA.108.802918**

contribution of TNFR1- and TNFR2-dependent inflammatory signaling in vivo. Our results establish that TNFR-specific effects in HF relate to both pathological remodeling and NF-κB activation, such that TNFR1 induces persistent NF-κB activation and accelerates remodeling, whereas TNFR2 counterbalances these effects. Moreover, these unique and divergent inflammatory responses specific to each TNFR in the failing heart suggest that global TNF inhibition, as was done in clinical trials, would abrogate both protective and detrimental effects.

Methods

Please see the expanded Methods in the online-only Data Supplement. All studies were performed in compliance with the National Institutes of Health *Guide for the Care and Use of Laboratory Animals* (Department of Health and Human Services publication NIH 85-23, revised 1996).

Mouse Models

Male mice aged 12 to 28 weeks were used (the Jackson Laboratories, Bar Harbor, Me). TNFR1$^{-/-}$ and TNFR2$^{-/-}$ mice were obtained from Jackson Laboratories (stock No. 002818 and No. 002620, respectively). The background strain, C57BL/6 (No. 000664), was used as wild-type (WT) control.

Coronary Ligation and Experimental Protocol

After the induction of anesthesia with tribromoethanol (0.25 mg/g IP), mice were intubated and supported with a MiniVent Mouse Ventilator (Harvard Apparatus), and anesthesia was maintained with 1% isoflurane. Under sterile conditions, the heart was exposed via a left thoracotomy in the fourth intercostal space. An 8.0 Prolene ligature was passed and tied around the proximal left coronary artery (HF group). In sham animals, the suture was passed but not tied. The chest was then closed with 5.0 silk. The total mice used were as follows: C57BL/6, n=90; TNFR1$^{-/-}$, n=46; and TNFR2$^{-/-}$, n=39. Mice were followed for 4 weeks after the operation. All TNFR1$^{-/-}$ and TNFR2$^{-/-}$ ligated mice and ≈50% WT ligated mice with premature death underwent autopsy to assess for blood in the chest cavity as an indicator of left ventricular (LV) rupture.

Echocardiography

Under tribromoethanol sedation, echocardiography was performed at baseline and 4 weeks with the use of a Philips Sonos 5500, 15-MHz linear array transducer. Measurements included LV end-diastolic and end-systolic diameter, wall thickness, and end-diastolic and end-systolic volume with the use of the modified Simpson's method.

LV Pressure Measurement

In a subset of mice, LV catheterization was performed 4 weeks after the operation as described previously[10] with the use of a Millar 1.4F pressure catheter (model SPR-835) inserted retrogradely via the right carotid artery. Systolic function was indexed by dP/dt_{max} and dP/dt_{max} normalized for instantaneous LV pressure. Diastolic function was assessed by LV end-diastolic pressure, and tau, the time constant of LV relaxation, was determined from the regression of dP/dt versus LV pressure.

Tissue Harvest

After the final study, mice were given sodium pentobarbital (50 mg/kg IP). The hearts were arrested in diastole with intravenous KCl, excised rapidly, and rinsed in ice-cold physiological saline. A short-axis LV section was formalin-fixed for 16 hours, dehydrated in ethanol, and paraffin-embedded for histological studies. The remaining LV was separated into infarcted (scar) and noninfarcted regions, snap-frozen in liquid nitrogen, and stored at −80°C. Unless otherwise specified, noninfarcted tissue was used for molecular analyses.

Cell Culture and Transfection

H9c2 cells (ATCC) were seeded in 100-mm tissue culture dishes and transfected for 24 hours with the plasmid DNA (5 μg per dish) with the use of Transfectin transfection reagent (BioRad, Hercules, Calif). Briefly, 10 μL of Transfectin was added to 500 μL of serum-free Dulbecco's modified Eagle's medium followed by the addition of plasmid DNA. The mixture was incubated for 15 minutes at room temperature before it was added onto the cells. In specific protocols, cells were also treated with 20 ng/mL of either recombinant mouse TNF or interleukin (IL)-1β (BD Biosciences) for different time periods as indicated.

Construction of Expression Plasmids

Expression plasmids for NF-κB subunits p65 and p50 were purchased from Panomics. Full-length mouse TNFR2 cDNA was amplified by polymerase chain reaction (PCR) from mouse aortic endothelial cell RNA with the use of the following primers: forward 5′-CACCGCCACCGCTGCCCCTATG-3′, reverse 5′-GTCAGGGGTCAGGCCACTTT-3′. The cDNA was cloned into pcDNA3.1-TOPO expression plasmid (Invitrogen, Carlsbad, Calif), and its sequence was verified. Truncated TNFR1 expression constructs (TNFR1Δ205 and TNFR1Δ244) were generous gifts from Drs Wang Min and Jordan Pober, Yale University.[11]

Western Immunoblotting

Total protein extraction, SDS-PAGE Western blotting, and immunodetection with the use of electrochemiluminescence were performed as described previously.[10,12,13]

Electrophoretic Mobility Shift Assay

NF-κB DNA binding activity was quantified by electrophoretic mobility shift assay (EMSA) as described previously.[12] To determine NF-κB subunit composition, we performed gel supershift assays. Nuclear protein (10 μg) was preincubated for 40 minutes on ice with antibodies against the NF-κB subunits p65, p50, p52, cRel, or Rel B (1 μg, Santa Cruz) or control IgG (1 μg) before the addition of the ^{32}P-labeled double-stranded consensus oligonucleotide.

Quantitative Real-Time PCR

Total RNA was isolated from LV tissue with TRIzol reagent (Invitrogen), and cDNA was synthesized from 1 μg RNA with the iScript cDNA Synthesis kit (BioRad). Relative levels of mRNA transcripts for atrial natriuretic factor, connective tissue growth factor, TNF, IL-1β, IL-6, IL-10, matrix metalloproteinase (MMP)-2, and MMP-9 were quantified by real-time PCR with the use of SYBR Green (Applied Biosystems, Foster City, Calif). Data were normalized to GAPDH expression by the $\Delta\Delta C_T$ comparative method.[14] Primer pairs are listed in Table I in the online-only Data Supplement.

Histology and Immunohistochemistry

Hematoxylin-eosin and Masson's trichrome stains were used to determine cardiomyocyte cross-sectional area and myocardial fibrosis. Immunostaining for malondialdehyde-adducted proteins was performed with the use of anti-malondialdehyde antibody (Academy Bio-Med) as described previously.[13] Activated macrophages were detected by rat anti-mouse MOMA-2 monoclonal antibody (Chemicon). Immunoreactivity was quantitated from at least 20 random fields by light microscopy. Apoptosis was assessed by terminal deoxytransferase–mediated dUTP nick-end labeling (TUNEL) with an APO-BrdU TUNEL Assay (Invitrogen). Sections were also costained with DAPI (Invitrogen) to identify nuclei and with mouse anti-α-actinin conjugated with TRITC (abcam) to identify myocytes. Images were recorded with a Zeiss SM510 inverted confocal scanning laser microscope.

Statistical Analysis

Several statistical techniques were used. For 2-group comparisons, we used the unpaired 2-sample *t* test. For comparisons of >2 groups, we used 1-way ANOVA if there was 1 independent variable (eg,

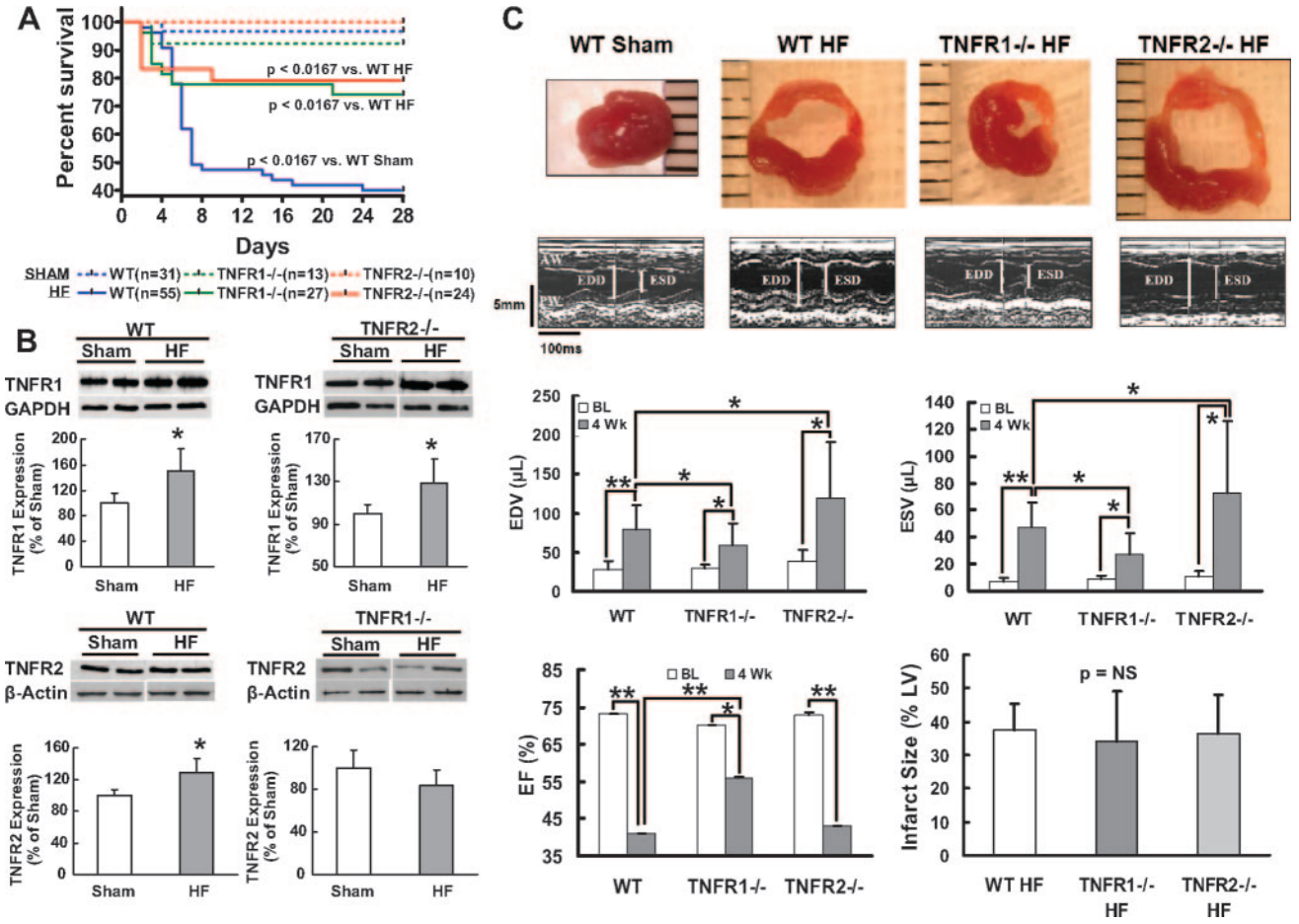

Figure 1. TNFR1 and TNFR2 differentially modulate LV remodeling. A, Kaplan–Meier survival curves from WT, TNFR1$^{-/-}$, and TNFR2$^{-/-}$ mice after coronary ligation (HF) or sham operation. B, Immunoblots and corresponding group data depicting changes in TNFR1 and TNFR2 expression in failing, remodeled myocardium. *P<0.05 vs sham. C, Short-axis LV sections, M-mode echocardiograms, and group data for LV function and infarct size from WT, TNFR1$^{-/-}$, and TNFR2$^{-/-}$ sham and HF mice. EDV indicates end-diastolic volume; ESV, end-systolic volume; EF, ejection fraction; and BL, baseline. **P<0.005, *P<0.05.

genotype alone), 2-way ANOVA if there were 2 independent variables (eg, genotype and ligation status), and 2-way repeated-measures ANOVA for matched observations over time with 2 independent variables. To adjust for multiple comparisons, we performed Student-Newman-Keuls post test, which maintains overall type I error (α) at 5%. Pairwise comparisons were made between sham groups across genotypes, sham versus HF groups within each genotype, and HF groups across genotypes. A probability value of <0.05 was considered significant.

Animal survival was evaluated by the Kaplan–Meier method, and the log-rank test was used to compare survival curves between WT sham and WT HF as well as between WT HF and TNFR1$^{-/-}$ and TNFR2$^{-/-}$ HF groups (testing 3 null hypotheses). Multiple testing Bonferroni adjustment was performed manually, and a probability value of <0.0167 (0.05/3) was considered significant. Continuous data are summarized as mean±SD.

The authors had full access to and take full responsibility for the integrity of the data. All authors have read and agree to the manuscript as written.

Results

TNFR1 and TNFR2 Differentially Modulate Postinfarction Remodeling

Echocardiography revealed no baseline differences in LV wall thickness or systolic function between WT, TNFR1$^{-/-}$, and TNFR2$^{-/-}$ mice (Table II in the online-only Data Supplement). TNFR2$^{-/-}$ mice had a mild increase in LV size over WT, consistent with the ≈15% greater body weight of these animals. In comparison with sham-operated mice, WT mice at 28 days after infarction exhibited significantly increased lung, right ventricular, and liver weight normalized for tibia length (TL), consistent with pulmonary and systemic congestion that are hallmarks of HF (sham versus HF, mg/mm: lung/TL, 6.7±1.1 versus 7.7±2.5, P<0.05; right ventricle/TL, 1.0±0.3 versus 1.3±0.4, P<0.005; liver/TL, 52.2±8.0 versus 57.0±8.2, P<0.05). Kaplan–Meier survival curves (Figure 1A) revealed significantly increased HF mortality over sham for each genotype at 28 days after infarction. Deficiency of either TNFR imparted a survival benefit over WT HF, occurring primarily in the first week after infarction. In this time frame after coronary ligation, cardiac rupture is the main cause of death and is associated with MMP-2 and MMP-9 activation.[15,16] In WT HF, the incidence of LV rupture was 45%, whereas no rupture was seen in either TNFR1$^{-/-}$ or TNFR2$^{-/-}$ HF mice. Moreover, at 4 weeks after infarction, there was markedly increased MMP-2 and MMP-9 gene expression in WT noninfarcted myocardium over sham, whereas there was no such upregulation in TNFR1$^{-/-}$ or TNFR2$^{-/-}$ HF hearts (Figure I in the online-only Data

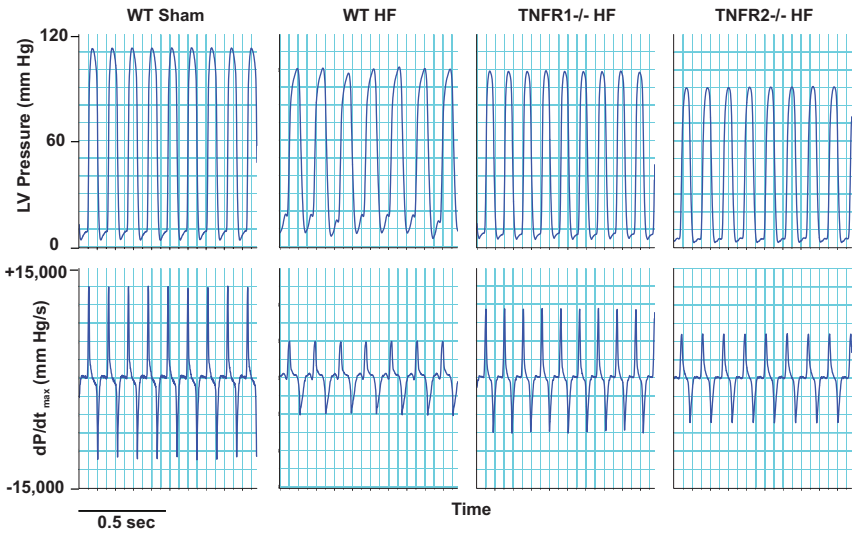

Figure 2. Representative hemodynamic recordings for LV pressure and dP/dt_{max} from WT sham, WT HF, $TNFR1^{-/-}$ HF, and $TNFR2^{-/-}$ HF mice. LV peak pressure and dP/dt_{max} were depressed and LVEDP was elevated in WT HF. $TNFR1^{-/-}$ HF displayed global improvement in these parameters. $TNFR2^{-/-}$ HF exhibited similar reductions in dP/dt_{max} but improved LV end-diastolic pressure compared with WT HF.

Supplement). In addition, in the infarct scar, $TNFR1^{-/-}$ and $TNFR2^{-/-}$ HF exhibited significantly attenuated MMP-2 and MMP-9 expression compared with WT HF. These results suggested that signaling via both TNFR1 and TNFR2 contributes to MMP induction and cardiac rupture after coronary ligation in mice.

In WT failing hearts (noninfarcted myocardium), TNFR1 and TNFR2 protein increased 1.5- and 1.3-fold, respectively, over sham (Figure 1B). In $TNFR2^{-/-}$ HF, TNFR1 also increased 1.5-fold, analogous to WT. However, in $TNFR1^{-/-}$ HF, there was no change in TNFR2. Figure 1C depicts LV tissue sections, M-mode echocardiograms, and corresponding group data. With HF, there was LV dilatation (increased LV end-diastolic volume and LV end-systolic volume) and systolic dysfunction (reduced LV ejection fraction) regardless of genotype. However, compared with WT HF, LV dilatation was attenuated in $TNFR1^{-/-}$ HF and exaggerated in $TNFR2^{-/-}$ HF. LV ejection fraction was also improved in $TNFR1^{-/-}$ HF; however, it was not different in $TNFR2^{-/-}$ HF despite the larger chamber volumes. Differences in LV remodeling occurred despite equivalent infarct size in WT, $TNFR1^{-/-}$, and $TNFR2^{-/-}$ HF, indicating divergent responses in the remote (noninfarcted) and border zones.

TNFR1 and TNFR2 Have Divergent Effects on Inotropy but Cooperatively Impair Lusitropy in HF

Figure 2 shows representative LV pressure and dP/dt tracings from WT sham and WT, $TNFR1^{-/-}$, and $TNFR2^{-/-}$ HF. Summary hemodynamic data from all groups are shown in the Table. WT failing hearts exhibited marked systolic and diastolic dysfunction over sham with reduced HR, LV systolic pressure, dP/dt_{max}, dP/dt_{max} normalized for instantaneous LV pressure, and increased LV end-diastolic pressure and tau. $TNFR1^{-/-}$ HF displayed uniform improvements in these parameters compared with WT HF, indicating better contractility and lusitropy. Interestingly, despite exaggerated remodeling, $TNFR2^{-/-}$ HF exhibited a mixed mechanical response. LVSP, dP/dt_{max}, and dP/dt_{max} normalized for instantaneous LV pressure were markedly depressed, comparable to WT HF. However, LVEDP and tau, indicators of diastolic performance, were much improved over WT HF. Taken together, this indicated that whereas TNFR1 deficiency in HF resulted in global improvement in systolic and diastolic function, TNFR2 deficiency exaggerated structural remodeling but still improved diastolic properties, thereby moderating changes in LV performance.

Table. LV Hemodynamics in WT, $TNFR1^{-/-}$ and $TNFR2^{-/-}$ Sham, and HF Mice

	WT		$TNFR1^{-/-}$		$TNFR2^{-/-}$	
	Sham (n=15)	HF (n=21)	Sham (n=7)	HF (n=11)	Sham (n=8)	HF (n=15)
Heart rate, bpm	539±50	431±49*	519±36	511±47‡	530±35	475±53*‡
LVPSP, mm Hg	98±8	86±8*	99±10	96±8‡	98±12	84±5*§
dP/dt_{max}, mm Hg/s	10245±2054	4962±1346*	9328±2084	7167±1426*‡	9611±1659	4997±993*§
dP/dt_{max}/IP, s^{-1}	185±35	98±22*	165±29	118±19*‡	170±34	101±22*§
LVEDP, mm Hg	8±3	16±4*	7±1	12±4*‡	9±3†	8±4‡§
Tau, ms	9.1±2.1	18.8±3.6*	10.4±2.9	14.0±2.3*‡	10.4±1.8	15.2±2.8*‡

All values are mean±SD. LVPSP indicates LV peak systolic pressure; dP/dt_{max}, maximal rate of change in LV pressure; dP/dt_{max}/IP, dP/dt_{max} normalized for instantaneous LV pressure; LVEDP, LV end-diastolic pressure; and tau, time constant of LV relaxation.

*$P<0.05$ vs respective sham.

†$P<0.05$ vs $TNFR1^{-/-}$.

‡$P<0.05$ vs WT HF.

§$P<0.05$ vs $TNFR1^{-/-}$ HF.

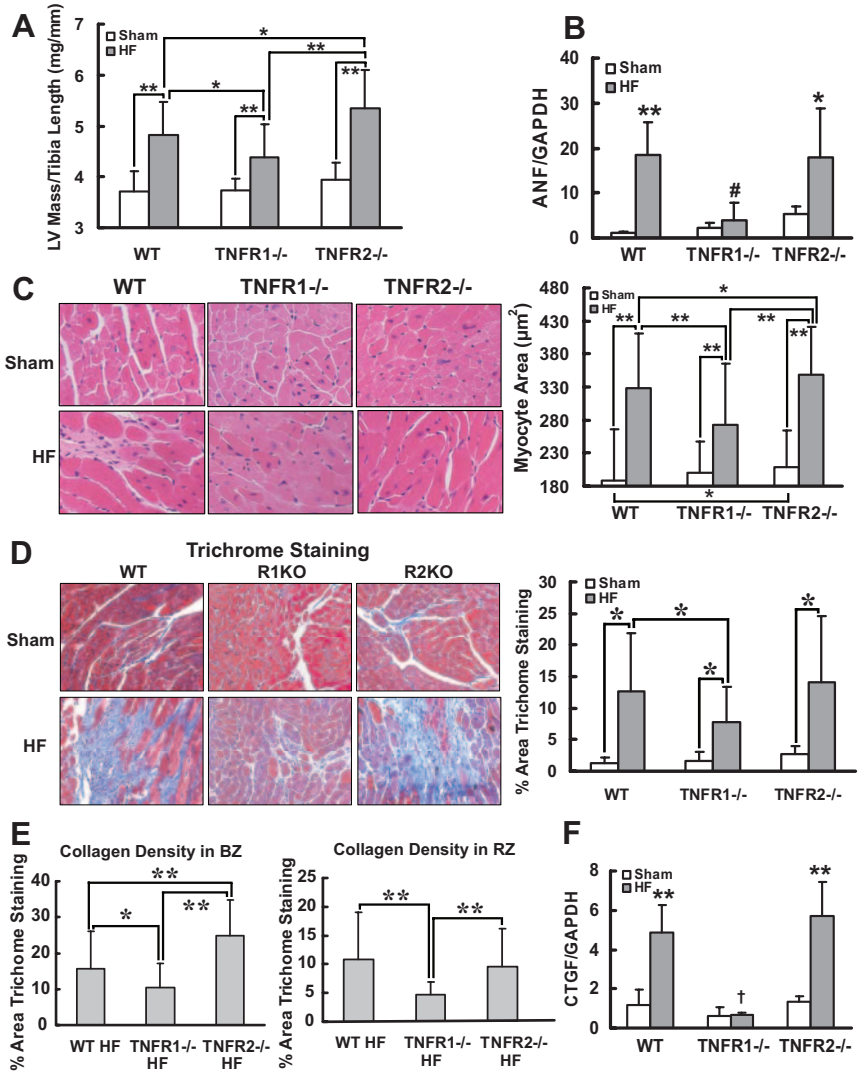

Figure 3. TNFR1- and TNFR2-specific effects on hypertrophy and fibrosis in HF. A, LV mass/TL ratio from WT, TNFR1$^{-/-}$, and TNFR2$^{-/-}$ sham and HF mice. $^{**}P<0.005$, $^{*}P<0.05$. B, Normalized atrial natriuretic factor (ANF) gene expression from sham and failing myocardium by quantitative RT-PCR analysis (n=4 per group). $^{**}P<0.005$, $^{*}P<0.05$ vs sham, $\#P<0.005$ vs WT and TNFR2$^{-/-}$ HF. C, Representative hematoxylin-eosin histomicrographs of remodeled myocardium from each experimental group and quantification of myocyte cross-sectional area. $^{**}P<0.0001$, $^{*}P<0.05$. D, Masson's trichrome stains and quantification of fibrosis in noninfarcted myocardium (ie, remote and border zones). R1KO indicates TNFR1 knockout; R2KO, TNFR2 knockout. $^{*}P<0.05$. E, Selective border zone (BZ) and remote zone (RZ) fibrosis quantification. $^{**}P<0.001$, $^{*}P<0.05$. F, Normalized connective tissue growth factor (CTGF) gene expression by quantitative RT-PCR. $^{**}P<0.005$ vs sham; $\dagger P<0.005$ vs WT and TNFR2$^{-/-}$ HF (n=6 per group).

TNFR1 and TNFR2 Differentially Modulate Cardiac Hypertrophy and Fibrosis in HF

Failing hearts from each HF group exhibited increased LV mass/TL ratio compared with sham, consistent with LV hypertrophy (Figure 3A). Compared with WT HF, the LV/TL ratio was lower in TNFR1$^{-/-}$ HF and higher in TNFR2$^{-/-}$ HF. Atrial natriuretic factor gene expression by reverse transcription (RT) PCR (Figure 3B) also revealed increased and comparable expression in WT and TNFR2$^{-/-}$ HF compared with TNFR1$^{-/-}$ HF (which was not significantly increased over TNFR1$^{-/-}$ sham). Consistent with the gravimetric data, histological assessment revealed larger myocyte area in all HF groups compared with sham, but the degree of hypertrophy was attenuated in TNFR1$^{-/-}$ HF and enhanced in TNFR2$^{-/-}$ HF (Figure 3C). These results suggested that in HF, TNFR1 is prohypertrophic, whereas TNFR2 is antihypertrophic.

Collagen deposition in noninfarcted myocardium (remote and border zones) was significantly augmented in the failing heart (Figure 3D). The degree of fibrosis was attenuated in TNFR1$^{-/-}$ HF compared with either WT or TNFR2$^{-/-}$ HF, both of which exhibited equivalent increases in fibrosis. Similar responses were seen for gene expression of connective tissue growth factor, a profibrotic matrix-associated protein (Figure 3F). Notably, compared with WT HF, border zone collagen was attenuated in TNFR1$^{-/-}$ HF mice but exaggerated in TNFR2$^{-/-}$ HF mice (Figure 3E). The pattern of remote zone collagen deposition was similar to that in total collagen deposition. This suggested that changes in border zone fibrosis in TNFR2$^{-/-}$ mice may have influenced scar stability and contributed to improvements in LV diastolic performance and survival over WT HF, despite exaggerated chamber dilatation and hypertrophy.

TNFR1 and TNFR2 Induce Divergent NF-κB Signaling Responses in HF

EMSA revealed marked NF-κB activation in failing myocardium (Figure 4A), and gel supershifts revealed that p65 was the primary NF-κB subunit, with a minor contribution from RelB and negligible p50, p52, and cRel. A similar supershift pattern was seen in both TNFR1$^{-/-}$ and TNFR2$^{-/-}$ HF hearts (data not shown). As seen in Figure 4B, WT failing hearts exhibited a robust (>2-fold) increase in NF-κB DNA binding compared with sham. Moreover, there was significant atten-

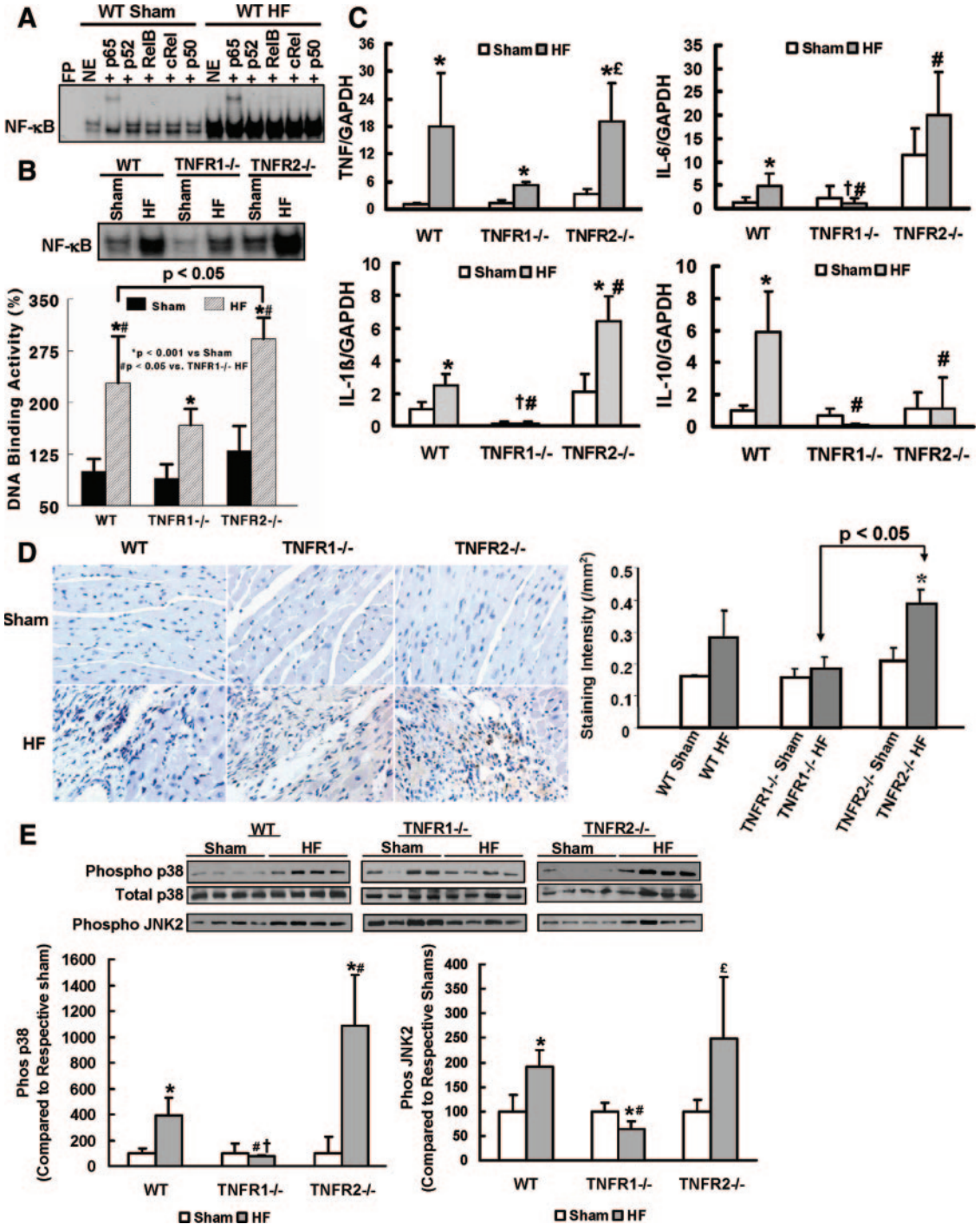

Figure 4. TNFR1 and TNFR2 induce divergent NF-κB and inflammatory signaling responses in HF. A, NF-κB DNA binding activity and subunit composition by EMSA and gel supershifts in nuclear extracts from WT sham and HF hearts. B, NF-κB DNA-binding activity in nuclear extracts from WT, TNFR1$^{-/-}$, and TNFR2$^{-/-}$ sham and HF hearts. C, Normalized gene expression of TNF, IL-1β, IL-6, and IL-10 by quantitative RT-PCR analysis (n=6 per group). D, Anti-MOMA-2 immunohistochemistry for activated macrophages (brown staining) in sham and failing hearts and corresponding quantification. E, Western blots and densitometry for phospho/total p38 and phospho (Phos)-JNK2 in sham and failing LV tissue. *P<0.05 vs sham, #P<0.05 vs WT HF, †P<0.05 vs TNFR2$^{-/-}$ HF, £P<0.05 vs TNFR1$^{-/-}$ HF.

uation of NF-κB activation in TNFR1$^{-/-}$ HF and, conversely, exaggeration of NF-κB activity in TNFR2$^{-/-}$ HF.

Cardiac gene expression (by RT-PCR) of proinflammatory TNF, IL-1β, and IL-6 and the antiinflammatory IL-10 was markedly increased in WT HF compared with sham (Figure 4C). This increase was either absent or attenuated in TNFR1$^{-/-}$ HF, suggesting a generalized reduction of inflammatory responses on loss of TNFR1 in HF. In TNFR2$^{-/-}$ HF, the upregulation of proinflammatory cytokines was either comparable to (TNF) or augmented over (IL-1β and IL-6) WT HF, whereas there was no increase at all in antiinflammatory IL-10. These results paralleled the changes in NF-κB

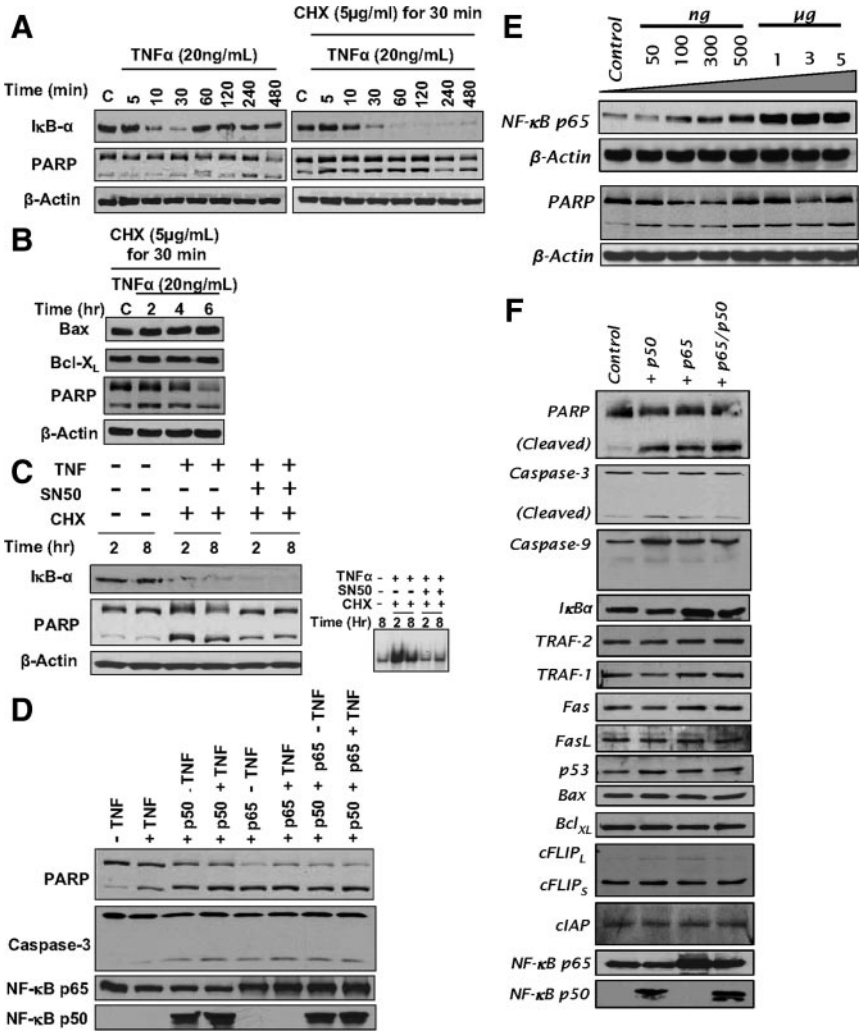

Figure 5. Sustained NF-κB activation is proapoptotic in H9c2 cardiomyocytes. A, H9c2 cells were treated with TNF with or without pretreatment with the protein synthesis inhibitor cycloheximide (CHX), and cell lysates were analyzed by Western blotting. TNF induced rapid IκBα degradation with resynthesis within 1 hour but no apoptosis, as indicated by predominantly uncleaved PARP. Cycloheximide pretreatment prevented IκBα resynthesis and induced apoptosis (augmented cleaved PARP). B, Bcl-X_L protein expression and the Bcl-X_L/Bax ratio with cycloheximide pretreatment and TNF stimulation. C, Preincubation with SN50, a peptide inhibitor of NF-κB nuclear translocation, attenuated apoptosis. D, H9c2 cells were transfected with either empty vector (pcDNA 3.1) or p65 and/or p50 expression vectors for 24 hours followed by treatment with or without TNF for 8 hours. Sustained p65 or p50 overexpression augmented PARP and caspase-3 cleavage, irrespective of TNF exposure. E, H9c2 cells were transfected for 24 hours with increasing amounts of p65 expression vector, and total amount of DNA was compensated with pcDNA3.1. The apoptotic effect of p65 exhibited dose dependency. F, H9c2 cells transfected with p65 and/or p50 for 24 hours did not exhibit changes in expression of a variety of proapoptotic and antiapoptotic proteins including TRAF-1 and -2, Fas and FasL, Bax and Bcl-X_L, cFLIP and cIAP, and p53. Results in A to F are representative of 4 independent experiments.

because TNF, IL-1β, and IL-6 are regulated by NF-κB and because IL-10 is a known suppressor of NF-κB activation. Moreover, compared with sham, there was increased MOMA-2 staining for activated macrophages in the myocardium of $TNFR2^{-/-}$ HF ($P<0.05$) and a trend toward increased staining in WT HF, but no change in $TNFR1^{-/-}$ HF (Figure 4D). $TNFR2^{-/-}$ HF also exhibited more activated macrophages than did $TNFR1^{-/-}$ HF ($P<0.05$). TNF-mediated activation of either JNK or p38 MAPK can also induce significant proinflammatory effects. WT HF exhibited augmented p38 MAPK and JNK2 phosphorylation over WT sham, both of which were attenuated in $TNFR1^{-/-}$ HF (Figure 4E). In $TNFR2^{-/-}$ HF, p38 MAPK phosphorylation was exaggerated, paralleling NF-κB activity, whereas JNK2 phosphorylation was comparable to WT HF. Taken together, these results indicate moderation and exacerbation of the HF-associated proinflammatory state on loss of TNFR1 or TNFR2, respectively.

Sustained NF-κB Activation Is Proapoptotic in H9c2 Cardiomyocytes, an Effect Modulated by TNFR1

In these studies, apoptosis was indexed by levels of cleaved poly-ADP ribose polymerase (PARP) and caspase-3. As shown in Figure 5A, TNF induced rapid IκBα degradation in H9c2 cells, with the appearance of newly synthesized IκBα within 1 hour, indicating transient NF-κB activation. There was no apoptosis, indicated by predominantly uncleaved PARP (top band). In contrast, pretreatment with the protein synthesis inhibitor cycloheximide before TNF prevented IκBα resynthesis and induced apoptosis (augmented cleaved PARP). Although the mechanism commonly invoked for TNF-induced apoptosis with cycloheximide is the prevention of synthesis of NF-κB–responsive antiapoptotic proteins,[15,25] protein expression of NF-κB–responsive Bcl-X_L and the Bcl-X_L/Bax ratio did not change (Figure 5B). In contrast, inhibition of NF-κB nuclear translocation by the peptide SN50 attenuated apoptosis (Figure 5C), suggesting that sustained NF-κB activity was itself contributing to cell death. Moreover, selective overexpression of p65 and/or p50 for 24 hours augmented PARP and caspase-3 cleavage, regardless of TNF exposure (Figure 5D), and the proapoptotic effect of p65 overexpression exhibited dose dependency (Figure 5E). Overexpression of p65 and/or p50 did not alter the expression of a range of proapoptotic and antiapoptotic proteins including TRAF-1 and -2, Fas and FasL, Bax and BCL_{XL}, cFLIP and cIAP, and p53 (Figure 5F), indicating separate, as of yet undetermined, mechanisms of NF-κB–induced cardiomyocyte apoptosis.

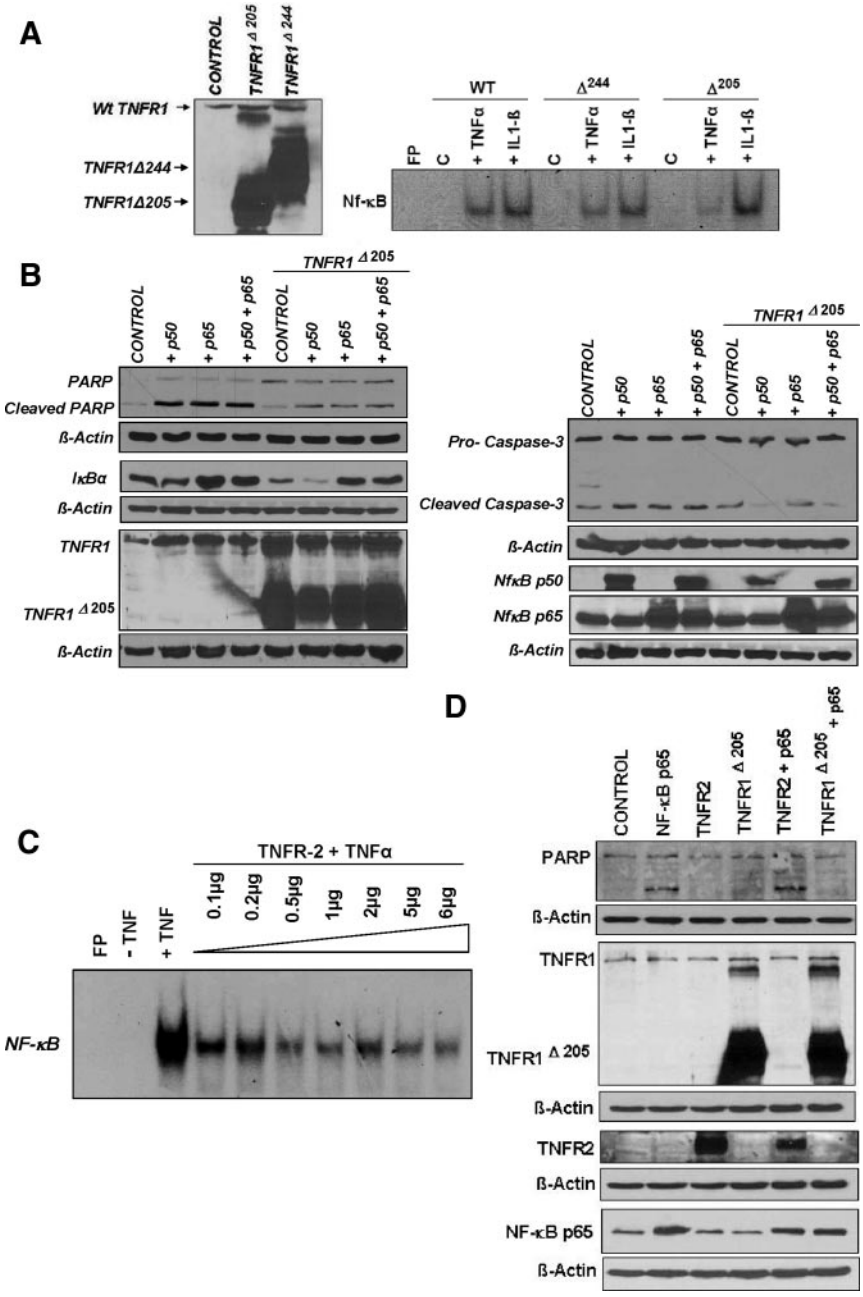

Figure 6. TNFR1 and TNFR2 uniquely modulate NF-κB activation. A, Left, H9c2 cells were transfected (5 μg) with either control vector (pcDNA3.1) or vectors encoding truncated human TNFR1 (TNFR1Δ244 or TNFR1Δ205) for 24 hours, and whole cell lysates were analyzed for TNFR1 expression by Western blotting. Right, similarly transfected cells were treated with either TNF or IL-1β for 30 minutes, and NF-κB DNA-binding activity was examined by EMSA. B, H9c2 cells were (co)transfected (6 μg) for 24 hours with p65 and/or p50 expression vectors and TNFR1Δ205. As indexed by PARP and caspase-3 cleavage, the proapoptotic effects of p65 and p50 were attenuated by TNFR1Δ205. C, H9c2 cells were transfected with increasing quantities of full-length TNFR2 for 24 hours followed by treatment with TNF for 30 minutes. Total amount of DNA (6 μg) was compensated with pcDNA3.1. EMSA revealed that TNFR2 overexpression reduced TNF-induced NF-κB activation in a dose-dependent manner. D, H9c2 cells were (co)transfected (5 μg) with vectors encoding p65 and/or TNFR2 for 24 hours. p65 and TNFR2 cotransfection did not reduce PARP cleavage. Results in A to D are representative of 3 independent experiments.

TNFR1 deletion mutants that lack most (TNFR1Δ244) or all (TNFR1Δ205) of the TNFR1 cytoplasmic domain,[12] as well as full-length, normally functional TNFR2, were overexpressed under similar conditions. TNFR1Δ205 was highly effective (and better than TNFR1Δ244) in abrogating NF-κB activation in response to TNF but not to IL-1β (Figure 6A). As shown in Figure 6B, the proapoptotic effects of p65 and p50 overexpression were markedly attenuated on TNFR1Δ205 cotransfection (indicated by diminished PARP and caspase-3 cleavage). TNFR1Δ205 overexpression also blunted the increase in IκBα, an NF-κB–responsive gene. Hence, NF-κB–induced apoptosis depends in part on TNF induction and TNFR1 downstream signaling. Conversely, TNFR2 overexpression dose-dependently reduced TNF-induced NF-κB activation (Figure 6C), consistent with the in vivo responses in HF (Figure 4). Cotransfection with both p65 and TNFR2 did not, however, reduce PARP cleavage and apoptosis in H9c2 cardiomyocytes (Figure 6D), suggesting that TNFR2 is a weaker modulator of NF-κB–induced apoptosis than TNFR1. This may not, however, fully represent the in vivo situation, given the complex binding properties of TNFR2 to membrane-bound and soluble TNF and the importance of juxtacrine interactions among different cell types in HF.

TNFR1 and TNFR2 Induce Divergent Apoptotic Effects but Similar Oxidative Stress Responses in the Failing Heart

Apoptosis, inflammation, and oxidative stress are 3 key TNF-mediated responses that are independently linked to pathological remodeling. Because our studies indicated that

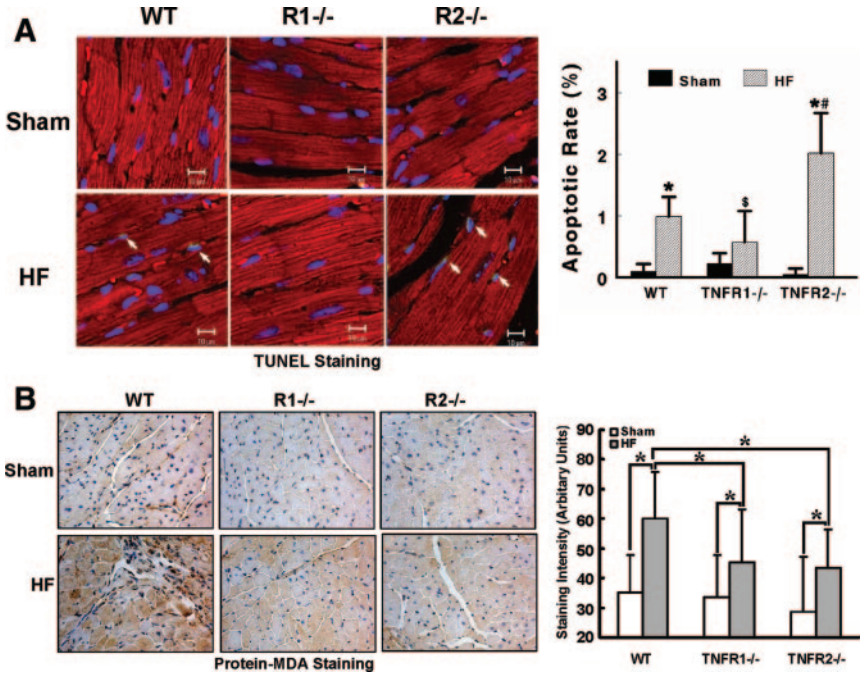

Figure 7. TNFR1 and TNFR2 induce divergent effects on apoptosis but similar effects on oxidative stress in HF. A, Apoptosis was quantified by APO-BrdU TUNEL assay in WT, TNFR1$^{-/-}$, and TNFR2$^{-/-}$ sham and HF hearts. Costaining was performed with α-actinin (red) to identify myocytes and DAPI (blue) to identify nuclei. Apoptotic nuclei are cyan (arrows). *$P<0.05$ vs sham, #$P<0.05$ vs WT HF, \$$P<0.05$ vs TNFR2$^{-/-}$ HF. B, Protein-malondialdehyde (MDA) immunostaining (brown staining) as an index of oxidative stress from the same experimental groups. *$P<0.05$, TNFR1$^{-/-}$ sham.

dichotomous NF-κB responses related to each TNFR could also differentially affect cell survival, we evaluated apoptosis in WT, TNFR1$^{-/-}$, and TNFR2$^{-/-}$ sham and HF hearts and whether changes in apoptosis were associated with directionally similar changes in oxidative stress. TUNEL staining revealed that apoptosis was increased over sham only in WT and TNFR2$^{-/-}$ HF and not in TNFR1$^{-/-}$ HF (Figure 7A), consistent with the cell data demonstrating a proapoptotic effect of TNFR1. Remarkably, TNFR2$^{-/-}$ HF hearts exhibited exaggerated apoptosis over WT and TNFR1$^{-/-}$ HF, indicating that TNFR2 confers (contrary to the cell studies) beneficial antiapoptotic effects in the failing heart. As shown in Figure 7B, immunostaining revealed a significant $\approx$2-fold increase in malondialdehyde-modified proteins in WT HF compared with sham. However, despite the marked differences in remodeling between TNFR1$^{-/-}$ and TNFR2$^{-/-}$ HF, there were similar reductions in oxidative stress compared with WT HF, suggesting that other factors such as apoptosis and inflammatory activation had primacy in the remodeling responses and that the changes in inflammation and apoptosis were not solely epiphenomena-related to a global improvement (or worsening) in LV remodeling.

Discussion

There are several key findings of this study. First, TNFR1- and TNFR2-dependent signaling had unique effects on postinfarction remodeling in vivo, such that TNFR1 aggravated, whereas TNFR2 ameliorated, chamber remodeling and hypertrophy. Second, the impact on cardiac mechanics and survival was more complex: Whereas TNFR1 and TNFR2 responses magnified and alleviated, respectively, LV systolic dysfunction, signaling through both receptors was necessary to increase postinfarction mortality (due to myocardial rupture) and to induce diastolic dysfunction. Third, TNFR1- and TNFR2-induced remodeling responses were accompanied by exacerbation and moderation of cardiac inflammation as assessed by NF-κB activation, inflammatory cytokine expression, p38 MAPK phosphorylation, and macrophage infiltration. Fourth, in H9c2 cardiomyocytes, TNFR1 augmented whereas TNFR2 moderated NF-κB activation, and sustained NF-κB activation was proapoptotic in a TNFR1-dependent manner. Fifth, TNFR1 was proapoptotic and TNFR2 antiapoptotic in the failing heart in vivo, whereas signaling via both receptors cooperatively augmented oxidative stress. Taken together, we have demonstrated complex pathophysiological responses in HF specific to each TNFR that are related in large part to disparate, opposing effects on NF-κB, inflammatory activation, and apoptosis. Analogous dichotomous TNFR-mediated responses in human HF may therefore help to explain the unexpectedly negative results of clinical trials of global TNF blockade.

Although the cytokine hypothesis posits a uniformly detrimental effect of TNF in HF, TNF has bimodal effects on contractility[17] and is cardioprotective during acute stress.[6–8] As shown in Figures 1B and 4C, TNF, TNFR1, and TNFR2 are all upregulated during the progression of remodeling in murine HF, indicating uniform enhancement of TNF signaling. This contrasts with end-stage human HF, in which TNF levels are high, but both TNFRs are downregulated.[18] Exacerbation of LV remodeling in TNFR2$^{-/-}$ HF mice occurred despite similar degrees of upregulation of both TNF and TNFR1, suggesting that unique cardioprotective benefits are referable to TNFR2 in HF. Moreover, amelioration of remodeling in TNFR1$^{-/-}$ HF mice occurred without an increase in TNFR2 expression and despite persistent (though attenuated) TNF upregulation, suggesting that detrimental biological responses in HF are uniquely referable to TNFR1. Thus, our results demonstrate that TNFR1 promotes detrimental remodeling, whereas TNFR2 is cardioprotective in HF with regard to chamber remodeling, systolic dysfunction, and hypertrophy.

These generalized effects on postinfarction remodeling notwithstanding, the complex functional interrelationship between the TNFRs in HF is evidenced by the cooperative, rather than divergent, effects of TNFR1 and TNFR2 on LV diastolic performance and survival as loss of signaling via either TNFR improved diastolic function and mortality after infarction. Prior studies have established that the most prevalent cause of death after infarction in mice is LV rupture (usually within the first week), that TNF directly contributes to cardiac rupture, and that this event is related to activation of MMPs, particularly MMP-2 and MMP-9, in the heart.[15,16] MMP-2 and MMP-9 activities increase by day 3, peak at day 7, and remain elevated to day 28 after infarction.[19] In our study, early LV rupture was prevented in both TNFR1$^{-/-}$ and TNFR2$^{-/-}$ HF mice, with both groups exhibiting less infarct and noninfarct zone MMP-2 and MMP-9 expression at 28 days compared with WT HF. This suggested that analogous MMP modulation with loss of either TNFR1 or TNFR2 function was also occurring at earlier time points after infarction, offering 1 potential mechanism for the reduced mortality in TNFR1$^{-/-}$ and TNFR2$^{-/-}$ mice. Hence, joint functionality of both TNF receptors was required for LV rupture to occur in the early postinfarction period. Notably, this mortality benefit was independent of the subsequent effects of TNFR1 and TNFR2 on LV remodeling. However, we speculate that the divergent TNFR-specific effects on progressive LV remodeling would secondarily affect mortality over extended periods of time after scar stabilization.

Because there was improved global remodeling in TNFR1$^{-/-}$ HF, accompanying improvements in diastolic function would be expected with TNFR1 deficiency. Indeed, there were generalized reductions in connective tissue growth factor expression and cardiac fibrosis in TNFR1$^{-/-}$ HF hearts, which would favorably influence LV diastolic properties. More difficult to reconcile is the maintenance of diastolic function in TNFR2$^{-/-}$ HF mice despite worsening of chamber remodeling. Because LV rupture was abrogated in these mice, these effects may be related to improved scar mechanics and/or border zone stability. Indeed, although the overall extent of cardiac fibrosis was similar in TNFR2$^{-/-}$ and WT HF, there was greater border zone collagen deposition that can potentially better resist rupture and favorably influence diastolic performance. However, it is important to recognize that the degree and distribution of myocardial fibrosis may itself also be influenced by altered global/regional wall stress, and whether the changes in connective tissue composition are a cause or consequence of altered chamber diastolic properties and wall stress is difficult to resolve with our experimental design.

A key finding of our study is that TNFR1 and TNFR2 had directionally opposite effects on NF-κB and inflammation in HF and that these events contributed to the differences in LV remodeling. TNFR1 recruits adaptor proteins via its death domain to trigger TRAF2-dependent signaling that activates NF-κB, JNK, and p38 MAPK.[9,20] TNFR2 can also activate NF-κB, JNK, and p38 MAPK via direct TRAF2 binding. TNF can also induce apoptosis via either TNFR and trigger the generation of reactive oxygen species.[9,20] We observed robust myocardial NF-κB activation in HF that was due almost entirely to p65. The failing heart also exhibited significant p38 and JNK2 activation, both of which have significant proinflammatory effects[21,22]; upregulation of proinflammatory TNF, IL-1β, and IL-6 and antiinflammatory IL-10; and enhanced tissue infiltration of activated macrophages, albeit at low absolute levels. Hence, there was a proinflammatory state in WT HF, consistent with prior studies.[1,18,23] In TNFR1$^{-/-}$ HF, there was attenuation of NF-κB activation, p38 and JNK phosphorylation, and TNF, IL-1β, IL-6, and IL-10 expression compared with WT HF, and no significant activated macrophage infiltration compared with TNFR1$^{-/-}$ sham. In contrast, TNFR2$^{-/-}$ HF hearts exhibited greater NF-κB activation, p38 MAPK phosphorylation, and IL-1β and IL-6 expression and less antiinflammatory IL-10 expression compared with WT HF, and greater activated macrophage infiltration than TNFR1$^{-/-}$ HF. Thus, our data establish that in chronic HF, TNFR1 is proinflammatory, whereas TNFR2 is antiinflammatory. Moreover, the sharp divergence of TNFR1 and TNFR2 effects on downstream mediators suggests that although acute signaling via the TNFRs may overlap significantly, TNFR crosstalk is much less prominent in chronic HF, leading to dichotomous downstream TNF responses.

Although NF-κB is chronically activated in HF,[24] whether this is protective or detrimental is unclear. In addition to stimulating inflammation, NF-κB upregulates both antiapoptotic and proapoptotic genes[9,20,25] and can potentially induce either survival or death. Our cell studies indicate that p65 and/or p50 overexpression is proapoptotic in H9c2 cardiomyocytes via a mechanism that appears independent of changes in classic proapoptotic and antiapoptotic gene expression. Moreover, analogous to in vivo HF, TNFR1 increased whereas TNFR2 blunted NF-κB activation. Importantly, the proapoptotic effects of NF-κB overexpression required TNF elaboration and concomitant TNFR1 signaling but were not modified by TNFR2 overexpression. Because HF is characterized by increases in both TNF/TNFRs and NF-κB, analogous functional interrelationships between TNFR1 and NF-κB may also occur in the failing heart. Indeed, evaluation of apoptotic rates revealed that in TNFR1$^{-/-}$ HF, attenuated NF-κB activation was paralleled by reduced myocardial apoptosis compared with WT HF, whereas the opposite response was seen in TNFR2$^{-/-}$ HF. Augmented myocardial TNF expression has been shown to increase oxidative protein modifications in the heart.[26] However, oxidative stress, as indexed by protein-malondialdehyde adducts, was equally reduced in both TNFR1$^{-/-}$ and TNFR2$^{-/-}$ HF, suggesting that the changes in cell survival were not simply epiphenomena accompanying global directional changes in remodeling. Hence, sustained changes in NF-κB activation are likely to underlie many of the divergent remodeling responses related to each TNFR. Indeed, recent studies indicate that postinfarction remodeling is attenuated in p50-null mice.[27,28] However, because our data show that NF-κB in the murine failing heart is almost entirely p65, further studies are required to define the relevance of these findings.

Our results extend as well as contrast with recent work in this area by others.[29,30] Ramani et al[29] also reported improved

remodeling and survival in TNFR1$^{-/-}$ mice after infarction over WT but no differences in TNF and IL-1β expression. Recently, after our original presentation of these data,[31] Monden et al[30] reported that TNFR1 ablation improved but TNFR2 ablation exacerbated postinfarction remodeling and IL-1β and IL-6 expression. Although these general conclusions are the same, there are also significant differences from our study, which establishes more complex effects of TNFR1 and TNFR2 in HF. Monden et al did not observe a postinfarction mortality benefit in TNFR2$^{-/-}$ mice or differences in LV rupture in either TNFR1$^{-/-}$ or TNFR2$^{-/-}$ mice. Moreover, we observed multifaceted hemodynamic responses in our study, with improved LV diastolic performance in TNFR2$^{-/-}$ HF mice despite exaggerated structural remodeling. In addition, unlike our results demonstrating a prohypertrophic and profibrotic effect of TNFR1 in the failing heart, Monden et al reported no effects of TNFR1 on these parameters. Although the reasons for these conflicting results are not fully clear, potential explanations include the older age of the mice and greater degrees of HF in WT mice (which exhibited a 2-fold higher LVEDP) in our study and perhaps an analytical approach that afforded greater discrimination of subtler differences between the genotypes. Further studies will be needed to resolve this. Most importantly, however, we provide novel mechanistic data that link in vivo remodeling to the primary downstream signaling pathways activated by TNF in the failing heart (particularly NF-κB), as well as to alterations in apoptosis and oxidative stress, and characterize the interrelationship between TNFR1, TNFR2, NF-κB, and cell survival. Indeed, our results indicate for the first time an opposing relationship between TNFR1 and TNFR2 and the activation of NF-κB in HF, and they help to provide a more comprehensive and mechanistic basis for TNFR-specific remodeling responses.

In summary, TNF induces dichotomous effects in HF that are directly referable to its 2 membrane receptors and occur (at least in part) as a result of disparate effects on the critical downstream mediator NF-κB, inflammatory signaling responses, and apoptosis. The overall balance between these opposing receptor-specific responses in turn determines the ultimate impact of TNF on the HF phenotype. Hence, these results provide a potential explanation for the failure of the anti-TNF clinical trials and, as a corollary, suggest that selective targeting of the individual TNFRs (TNFR1 blockade and/or TNFR2 augmentation) represents a better therapeutic approach in HF.

Sources of Funding

This work was supported by a Veterans Affairs Merit Award and National Institutes of Health grants ES11860, HL078825, and HL065660.

Disclosures

None.

References

1. Mann DL. Inflammatory mediators and the failing heart: past, present, and the foreseeable future. *Circ Res*. 2002;91:988–998.
2. Bozkurt B, Kribbs SB, Clubb FJ, Michael LH, Didenko VV, Hornsby PJ, Seta Y, Oral H, Spinale FG, Mann DL. Pathophysiologically relevant concentrations of tumor necrosis factor-α promote progressive left ventricular dysfunction and remodeling in rats. *Circulation*. 1998;97:1382–1391.
3. Li YY, Feng YQ, Kadokami T, McTiernan CF, Draviam R, Watkins SC, Feldman AM. Myocardial extracellular matrix remodeling in transgenic mice overexpressing tumor necrosis factor-α can be modulated by anti-tumor necrosis factor-α therapy. *Proc Natl Acad Sci U S A*. 2000;97:12746–12751.
4. Moe GW, Marin-Garcia J, Konig A, Goldenthal M, Lu X, Feng Q. In vivo TNF-α inhibition ameliorates cardiac mitochondrial dysfunction, oxidative stress, and apoptosis in experimental heart failure. *Am J Physiol*. 2004;287:H1813–H1820.
5. Iversen PO, Nicolaysen G, Sioud M. DNA enzyme targeting TNF-α mRNA improves hemodynamic performance in rats with postinfarction heart failure. *Am J Physiol*. 2001;281:H2211–H2217.
6. Kurrelmeyer K, Michael L, Baumgarten G, Taffet G, Peschon J, Sivasubramanian N, Mann DL. Endogenous myocardial tumor necrosis factor protects the adult cardiac myocyte against ischemic-induced apoptosis in a murine model of acute myocardial infarction. *Proc Natl Acad Sci U S A*. 2000;290:5456–5461.
7. Skyschally A, Gres P, Hoffmann S, Haude M, Erbel R, Schulz R, Heusch G. Bidirectional role of tumor necrosis factor-α in coronary microembolization: progressive contractile dysfunction versus delayed protection against infarction. *Circ Res*. 2007;100:140–146.
8. Wada H, Saito K, Kanda T, Kobayashi I, Fujii H, Fujigaki S, Maekawa N, Takatsu H, Fujiwara H, Sekikawa K, Seishima M. Tumor necrosis factor-α (TNF-α) plays a protective role in acute viral myocarditis in mice: a study using mice lacking TNF-α. *Circulation*. 2001;103:743–749.
9. Aggarwal BB. Signalling pathways of the TNF superfamily: a double-edged sword. *Nat Rev Immunol*. 2003;3:745–756.
10. Luo J, Hill BG, Gu Y, Cai J, Srivastava S, Bhatnagar A, Prabhu SD. Mechanisms of acrolein-induced myocardial dysfunction: implications for environmental and endogenous aldehyde exposure. *Am J Physiol*. 2007;293:H3673–H3684.
11. Zhang H, Zhang R, Luo Y, D'Alessio A, Pober JS, Min W. AIP1/DAB2IP, a novel member of the Ras-GAP family, transduces TRAF2-induced ASK1-JNK activation. *J Biol Chem*. 2004;279:44955–44965.
12. Chandrasekar B, Marelli-Berg FM, Tone M, Bysani S, Prabhu SD, Murray DR. Isoproterenol induces interleukin-18 expression via β2-AR, PI3 kinase, Akt, IκB kinase, and nuclear factor-κB signaling. *Biochem Biophys Res Commun*. 2004;319:304–311.
13. Srivastava S, Chandrasekar B, Gu Y, Luo J, Hamid T, Hill BG, Prabhu SD. Downregulation of CuZn-superoxide dismutase contributes to β-adrenergic receptor-mediated oxidative stress in the heart. *Cardiovasc Res*. 2007;74:445–455.
14. Livak KJ, Schmittgen TD. Analysis of relative gene expression data using real-time quantitative PCR and the 2-DDCT method. *Methods*. 2001;25:402–408.
15. Sun M, Dawood F, Wen WH, Chen M, Dixon I, Kirshenbaum LA, Liu PP. Excessive tumor necrosis factor activation after infarction contributes to susceptibility of myocardial rupture and left ventricular dysfunction. *Circulation*. 2004;110:3221–3228.
16. Matsumura S, Iwanaga S, Mochizuki S, Okamoto H, Ogawa S, Okada Y. Targeted deletion or pharmacological inhibition of MMP-2 prevents cardiac rupture after myocardial infarction in mice. *J Clin Invest*. 2005;115:599–609.
17. Prabhu SD. Cytokine-induced modulation of cardiac function. *Circ Res*. 2004;95:1140–1153.
18. Torre-Amione G, Kapadia S, Lee J, Durand J-B, Bies RD, Young JB, Mann DL. TNF-α and tumor necrosis factor receptors in the failing human heart. *Circulation*. 1996;93:704–711.
19. Mukherjee R, Mingoia JT, Bruce JA, Austin JS, Stroud RE, Escobar GP, McClister DM Jr, Allen CM, Alfonso-Jaume MA, Fini ME, Lovett DH, Spinale FG. Selective spatiotemporal induction of matrix metalloproteinase-2 and matrix metalloproteinase-9 transcription after myocardial infarction. *Am J Physiol*. 2006;291:H2216–H2228.
20. Wajant H, Pfizenmaier K, Scheurich P. Tumor necrosis factor signaling. *Cell Death Differ*. 2003;10:45–65.
21. Kyriakis JM, Avruch J. Mammalian mitogen-activated protein kinase signal transduction pathways activated by stress and inflammation. *Physiol Rev*. 2001;81:807–869.
22. Johnson GL, Nakamura K. The c-jun kinase/stress-activated pathway: regulation, function and role in human disease. *Biochim Biophys Acta*. 2007;1773:1341–1348.

23. Prabhu SD, Chandrasekar B, Murray DR, Freeman GL. β-Adrenergic blockade in developing heart failure: effects on myocardial inflammatory cytokines, nitric oxide, and remodeling. *Circulation*. 2000;101: 2103–2109.
24. Wong SC, Fukuchi M, Melnyk P, Rodger I, Giaid A. Induction of cyclooxygenase-2 and activation of nuclear factor-κB in myocardium of patients with congestive heart failure. *Circulation*. 1998;98:100–103.
25. Luo JL, Kamata H, Karin M. IKK/NF-κB signaling: balancing life and death—a new approach to cancer therapy. *J Clin Invest*. 2005;115: 2625–2632.
26. Canton M, Skyschally A, Menabò R, Boengler K, Gres P, Schulz R, Haude M, Erbel R, Di Lisa F, Heusch G. Oxidative modification of tropomyosin and myocardial dysfunction following coronary microembolization. *Eur Heart J*. 2006;27:875–881.
27. Frantz S, Hu K, Bayer B, Gerondakis S, Strotmann J, Adamek A, Ertl G, Bauersachs J. Absence of NF-κB subunit p50 improves heart failure after myocardial infarction. *FASEB J*. 2006;20:1918–1920.
28. Kawano S, Kubota T, Monden Y, Tsutsumi T, Inoue T, Kawamura N, Tsutsui H, Sunagawa K. Blockade of NF-κB improves cardiac function and survival after myocardial infarction. *Am J Physiol*. 2006;291: H1337–H1344.
29. Ramani R, Mathier M, Wang P, Gibson G, Tögel S, Dawson J, Bauer A, Alber S, Watkins SC, McTiernan CF, Feldman AM. Inhibition of tumor necrosis factor receptor-1-mediated pathways has beneficial effects in a murine model of postischemic remodeling. *Am J Physiol*. 2004;287: H1369–H1377.
30. Monden Y, Kubota T, Inoue T, Tsutsumi T, Kawano S, Ide T, Tsutsui H, Sunagawa K. Tumor necrosis factor-α is toxic via receptor 1 and protective via receptor 2 in a murine model of myocardial infarction. *Am J Physiol*. 2007;293:H743–H753.
31. Hamid T, Gu Y, Ortines RV, Luo J, Bhattacharya C, Xuan YT, Prabhu SD. Tumor necrosis factor (TNF) receptor1- and receptor2-dependent pathways differentially modulate post-infarction LV remodeling. *Circulation*. 2005;112:II-850. Abstract.

CLINICAL PERSPECTIVE

Despite the seminal observation that tumor necrosis factor-α (TNF) is an important mediator of pathological left ventricular remodeling in heart failure (HF), this discovery has not resulted in the development of new, effective treatments. On the contrary, the unexpected failure of clinical trials of global TNF blockade casts doubt on the precise roles of inflammatory activation in general and of TNF in particular in the progression of chronic HF. Because there are 2 cell-surface receptors for TNF (TNFR1 and TNFR2), we evaluated the remodeling responses specifically referable to each TNFR in chronic ischemic HF in vivo using TNFR1- and TNFR2-null mice. Our results indicate that TNF induces dichotomous effects in HF such that TNFR1 aggravated, whereas TNFR2 ameliorated, chamber remodeling and hypertrophy. Moreover, these effects occurred, at least in part, because of divergent effects on the activation of the downstream signaling mediator nuclear factor-κB, the regulation of inflammatory cytokines, and the induction of apoptosis: TNFR1 exacerbated, whereas TNFR2 ameliorated, these events. These results suggest that the overall balance between these opposing receptor-specific responses determines the ultimate impact of TNF on the HF phenotype and that analogous TNFR-specific effects in human HF should be considered when anti-TNF therapies are developed. Dichotomous TNFR-specific effects may also provide an explanation for the failure of the anti-TNF clinical trials. Selective targeting of the individual TNFRs (TNFR1 blockade and/or TNFR2 augmentation) may represent a better therapeutic approach in HF.